

# Thermal analysis of nanostructured calcite crystals covered with fatty acids

Karolina Kędra-Królik · Małgorzata Wszelaka-Rylik · Paweł Gierycz

CCTA10 Special Issue  
© Akadémiai Kiadó, Budapest, Hungary 2010

**Abstract** The way of precipitation process conducting is crucial for the final product properties and its further applications. In present experiments, the  $\text{CaCO}_3$  powders, produced by controlled fast precipitation trough gaseous  $\text{CO}_2$  absorption in  $\text{Ca}(\text{OH})_2$  slurry, have been covered by two fatty acids: dodecanoic (lauric) acid and tetradecanoic (myristic) acid. This multiphase reaction was conducted in a new rotating disc reactor unit which enables to control inter- and intra-face mass and energy transfer as well as the macro- and micromixing effects in the reacting system. The obtained nanopowders have been observed by the use of the scanning electron microscope. The X-ray diffraction technique as well as the dynamic light scattering (DLS) and the thermogravimetric method (TG) were further used for its deep analyses. The experimental data have allowed for distinction between different fatty acid molecules species present on calcite surface (chemisorbed ones, inter-located between adsorbed to surface, formed mono- and bilayers and the soap) or free fatty acids molecules if presented in the sample. The amount of fatty acid species forming different layers on calcite as well as the size and distribution of fatty acid coated  $\text{CaCO}_3$  powders have been also calculated.

**Keywords** Nanostructured calcite crystals · Dodecanoic (lauric) acid · Tetradecanoic (myristic) acid · Fatty acid-coated calcite · Thermal analysis

## Introduction

Calcium carbonate formation and aggregation processes have been studied from many years and are widely described in the literature [1–13]. However, the mechanism of the process is not fully understood till now and still investigated due to its increasing applications in commercial production of paper, paints, textiles, pharmaceuticals, and many others.

The crucial problem concerning the fabrication of functional solids is the proper, fully controlled precipitation. Although a lot of investigations have been done and described in the literature [1–16], there are still many questions about the full mechanism of crystals nucleation, growth as well as aggregation of freshly precipitated particles. In general, there are two basic mechanisms of crystals growth described in literature [1, 14]. The Ostwald approach which assumes that the larger crystals formation grows from smaller crystals which have higher solubility than larger ones (the smaller crystals act as fuel for the growth of bigger ones) and so-called “nonclassical crystallization mechanism by aggregation,” i.e., coalescence of initially stabilized nanocrystals which grow together and form one bigger particle [14, 17]. Adsorption of ions and organic molecules as well as the dehydration between coherent interfaces [14, 18] play also very important role in the oriented aggregation. There are some papers dealing with calcium carbonate formation through oriented aggregation of nanocrystals [17, 19]. Judat and Kind [14] described also the mechanism of crystal growth through self-assembled aggregation of nanometric crystallites followed by a fast recrystallization process. This way of particles formation control to fabricate ordered structures is inspired by processes observed in biological systems, and is one of the major topics of modern colloid and materials chemistry [14, 17, 19].

K. Kędra-Królik · M. Wszelaka-Rylik · P. Gierycz (✉)  
Institute of Physical Chemistry of Polish Academy of Science,  
44/52 Kasprzaka, 01-224 Warsaw, Poland  
e-mail: gierycz@ichf.edu.pl

In recent years, many research groups have dealt with application of organic additives as a template to produce inorganic materials and conduction of reaction in a macro- or microemulsions or in sol–gel matrixes [20–22]. Such methods give an opportunity to control of precipitation process or to modify product properties. There are also many ways of  $\text{CaCO}_3$  precipitation conducting without any additives [1–11, 23–25].

The production of inorganic nanomaterials cover by organic substances found nowadays wide industrial applications as pharmaceutics and semi-permeable membranes working as biosensors. The lipid self-assembled monolayers as supported membranes have attracted great attention as functionalizing methods of inorganic particles [20–22]. Such supramolecular structures combine the properties both from the particle core and lipid vesicle. As a result, we obtain stabilized deposited membrane which takes the architectural advantages of particles and the properties of lipid. This explains wide range of applications of solids coated with lipid layers in biotechnology or biomedicine.

The main objective of this study is to obtain and characterize calcium carbonate nanoparticles covered with dodecanoic (lauric) acid and tetradecanoic (myristic) acid layers. It can be done in two steps: first, it is necessary to prepare in a controlled way nanoparticles which will be used as solid supports for depositing lipid layers and, second, it is necessary to cover those particles with the fatty acids and determine their structure.

## Experimental

### Materials and solutions

Carbon dioxide used in experiments was taken directly from a gas bottle (99.9993% pure, from Linde) and calcium hydroxide from a pure sample (p. a. from POCH Gliwice, Poland). Both chemicals were used without any further purification. All solutions were prepared using doubly distilled and deionized water.

The initial concentration of calcium hydroxide used for experiments was equal to 56 mM. For this concentration, the largest (most developed) surface of  $\text{CaCO}_3$  is obtained [23] in our disc reactor [23–25]. The slurries (56 mM) were prepared by dispersing the weighted amount of 4 g of  $\text{Ca}(\text{OH})_2$  powder into deionized water in a 1  $\text{dcm}^3$  volumetric flask and then well-mixed. After 2 days, the slurry was treated with ultrasonic bath for 15 min, after that solution was thermostated in 298.15 K and immediately used for experiments.

The both fatty acids used in the experiment were taken directly from the following pure samples: dodecanoic (lauric) acid from 99% pure Sigma and tetradecanoic

(myristic) acid from 99 to 100% pure Sigma. The ethanol used for preparation of fatty acid solutions was taken from a pure sample (Chempur 96%).

### Precipitation and fatty acids covering procedures

Preparation of solid particles with defined crystal structures and a well-defined size distribution is based on a continuous formation of thin liquid films at the surface of the rotating discs where the mass transfer proceeds in diffusion–convective way. Rotating disc precipitation reactor allows conducting gas–liquid–solid reactions with controlled reagent transfer from gaseous to liquid phase, or reverse, and it can operate under batch or continuous mode [23–25].

The reactor chamber used in the experiments had a maximum volume of liquid reactant equal to 2  $\text{dcm}^3$ . Before each experiment, the reactor elements were cleaned with 10% HCl solution to get rid of any  $\text{CaCO}_3$  particles and then rinsed with deionized water. All processes were performed under atmospheric pressure and the constant temperature of the solution equal to 298.15 K. Gas inflow to the reactor was 2  $\text{dcm}^3 \text{ min}^{-1}$ , and was maintained at a constant level by Mass Flow Controller GFC (Aalborg) calibrated on  $\text{CO}_2$ .

The reaction kinetics was controlled by discs revolution speed rate equal to 120 revolutions per min (rpm) and the carbonation process was stopped when reacting solution reached  $\text{pH} = 7.5$  when the whole amount of calcium hydroxide has been converted into  $\text{CaCO}_3$  [23–25].

After finishing the carbonation process, the final solution (suspension of pure  $\text{CaCO}_3$ ) was mixed and stored into 6 (each 100 ml) flasks. At the mean time, three following different solutions of both lauric and myristic acids in ethanol have been prepared:

- (1) 10 mM of fatty acid per 1 gram of obtained pure  $\text{CaCO}_3$ —the concentration equal to the theoretically calculated concentration needed for covering of the whole  $\text{CaCO}_3$  surface by 0.5 alkyl monolayer,
- (2) 20 mM of fatty acid per 1 gram of obtained pure  $\text{CaCO}_3$ —the concentration equal to the theoretically calculated concentration needed for covering of the whole  $\text{CaCO}_3$  surface by 1 alkyl monolayer, and
- (3) 30 mM of fatty acid per 1 gram of obtained pure  $\text{CaCO}_3$ —the concentration equal to the theoretically calculated concentration needed for covering of the whole  $\text{CaCO}_3$  surface by 1.5 alkyl monolayer.

Then, 5 mL of the prepared fatty acids solutions were properly injected into each flasks and shook for 30 min. At the end of the experiment, the precipitated solids were collected by filtering through membrane filters (0.1  $\mu\text{m}$ ), washing by the distilled water, dried in 343.15 K, and

stored in vacuum oven (vacuum ca. 0.05 MPa). Such prepared powder was further investigated using thermogravimetric analysis.

### Characterization techniques

The pH changes during the course of reactions were measured by the combined glass electrode (EPP-3 for sewage and ultra pure water, Elmetron, Poland). The pH-meter was coupled with PC, and the experimental data were collected every second for carbonation time adjustment. EPP-3 was standardized before each experiment with three buffer solutions (pH at 298.15 K equal to 7.0, 10.0, and 11.85).

X-ray diffraction (XRD) patterns were collected on Bruker AXS D8 Advance powder diffractometer with Cu K $\alpha$  radiation. The  $2\theta$  (range from  $20^\circ$  to  $100^\circ$ ) with step  $0.1^\circ$  and time step 1 s were selected to analyze the CaCO<sub>3</sub> crystals structure and to estimate the crystallite size by means of the Scherrer equation from the full width of the half-maximum of the X-ray diffraction peak [26].

The particles size of pure and fatty acid covered CaCO<sub>3</sub> was examined with Zeta Plus instrument (Brookhaven Instruments Co.), which applies dynamic light scattering method for determination of effective diameter of particles and multimodal size distribution. For these measurements, in the case of CaCO<sub>3</sub>, a suspension of 30 mg of obtained and dried powder in 30 mL solution of  $10^{-3}$  M NaCl was prepared and in the case of fatty acid covered CaCO<sub>3</sub>, a suspension of 30 mg of obtained, and dried powder in 30 mL solution of 96% ethanol was prepared. They were sonicated for 5 s and immediately after that taken to analysis. The same probe was simultaneously examined for pure CaCO<sub>3</sub> with Turbiscan Lab instrument (Formulaction) which calculated the approximate particles diameter from the sedimentation kinetics analysis. For this purpose, the transmittance profiles of electroluminescent diode light ( $\lambda_{\text{air}} = 880$  nm) of the 55 mm high probe in glass cell were taken every minute through an hour. The computed diameter is the hydrodynamic diameter calculated from the Stokes law for concentrated dispersions [27].

For pure CaCO<sub>3</sub> crystals morphology, size, and aggregation examination, the SEM photographs of the probes were taken with Scanning Electron Microscope (Hitachi S 5500 SEM/STEM with cold field emission gun).

The surface analyses both for pure and fatty acids covered CaCO<sub>3</sub> were carried out from sorptometric analysis using Sorptomat ASAP 2405, Micrometrics Inc. The specific surface area of precipitated powders was calculated using Brunauer–Emmet–Teller (BET) adsorption isotherms and the pore size distribution by the use of the Barrett–Joyner–Halenda (BJH) method.

Thermogravimetric analysis (TG) of calcite treated with different amounts of fatty acids, have been done by the use of 951 TGA Du Pont Instruments in temperature range from 298.15 to 898.15 K. It allowed for adsorbed lipid layers morphology studies as well as for interface chemical composition and quantity examination. Obtained data gave possibility of distinction between different fatty acid molecules species present on calcite surface (chemisorbed ones, inter-located between adsorbed to surface, formed mono-, and bilayers and the soap) or free fatty acids molecules if presented in the sample. The amount of fatty acid species forming layers on calcite were calculated from TG data after peaks deconvolution.

## Results

### Reaction kinetics and pure CaCO<sub>3</sub> size and morphology

In the Ca(OH)<sub>2</sub>–H<sub>2</sub>O–CO<sub>2</sub> system, the reactive precipitation proceeds with a high rate if interface area is developed enough for high gas absorption and reaches high degree of supersaturation. Another important factor for super fine particles production is good macromixing conditions in the system to provide uniform spatial concentration distributions in bulk slurry [28].

Our investigations confirm that the fast precipitation occurs in the system with the rotating disc reactor (RDR) as a processing unit. The scheme of the reacting unit as well as the processes conducted in RDR during calcium carbonate precipitation for different initial Ca(OH)<sub>2</sub> concentration, discs revolution speed rate, or gas–liquid reagents interface have been published previously [23–25]. The higher mixing rate affects reaction time and, when mixing rate reaches about 100 rpm, the time is reduced twice in reference to 30 rpm [23]. Carbonation time is up to 10 min shorter for 56 mM, 0.12 m<sup>2</sup>/L reacting system. However, further increase of discs revolution speed rate, to 180 rpm, causes lower effect making the reaction time up to 2 min shorter [23]. That is, why in our investigations we have used the discs speed revolution equal to 120, initial concentration of Ca(OH)<sub>2</sub> equal to 56 mM and CO<sub>2</sub> flow equal to 2 dcm<sup>3</sup> per min. The reaction was led under atmospheric pressure at temperature equal to 298.15 K.

The distributions of particles size in suspensions are shown in Fig. 1. The obtained particles are almost monodispersive with mean diameter equal to 219 nm ( $\pm 5$  nm). Figure 2 presents the SEM micrograph of powders obtained for this suspension. One can see that CaCO<sub>3</sub> crystals form ordered aggregates of crystallites. Particles which form closely packed agglomerates are characterized by well-developed rhombohedral morphology. The single crystallite size is evidently much lower (<50 nm) than

results from DLS and the obtained powder looks very uniform in size and morphology.

The sedimentation kinetics [23] confirms the above results. There is no big aggregate in the precipitated powder. No migrations of particles were observed in any probe for about 20 min after suspension preparation and after this time of stability the particles agglomerate and when are dense enough start to sediment [23].

The XRD testing shows that the polymorphic modification of obtained  $\text{CaCO}_3$  powder is very pure and single calcite. In Fig. 3, the experimental reflexes suit very well to the standard calcite data (the black bars on the diagram). Therefore, in investigated system, the most thermodynamically stable structure is formed. It agrees with the previous data [23–25] where independent of the mixing rate in RDR or the initial concentration of calcium hydroxide always calcite was obtained. This is not a common result because usually under room temperature, the precipitate is a mixture of two or three  $\text{CaCO}_3$  polymorphs [29, 30]. The approximation of crystallite diameter

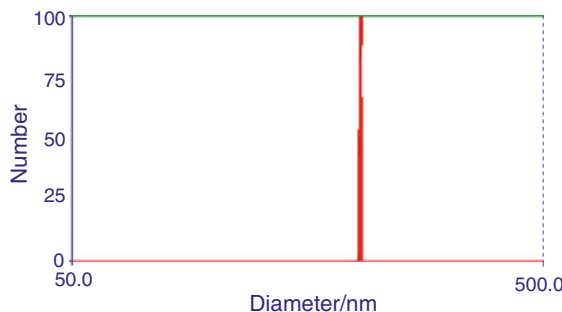


**Fig. 1** Particles size distribution from the DLS method for  $\text{CaCO}_3$  precipitated in RDR for initial  $\text{Ca}(\text{OH})_2$  concentration equal to 56 mM (mean diameter 219 nm)

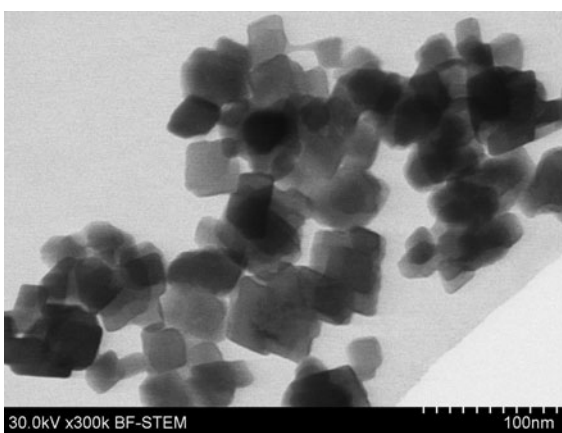


**Fig. 2** SEM picture of  $\text{CaCO}_3$  powders precipitated in RDR for initial  $\text{Ca}(\text{OH})_2$  concentration equal to 56 mM and rate of discs rotation equal to 120 rpm

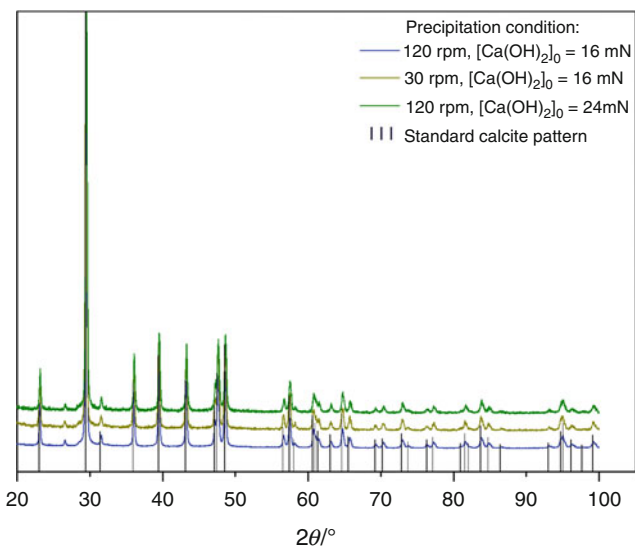


**Fig. 3** The X-ray diffraction patterns of  $\text{CaCO}_3$  samples precipitated in RDR for initial  $\text{Ca}(\text{OH})_2$  concentration equal to 56 mM and rate of discs rotation speed equal to 120 rpm together with standard calcite data

from the X-ray diffraction patterns using Scherrer equation for diffraction peaks (104 faces) gave values from about 25–35 nm ( $\pm 3$  nm). The differences between calculated values are not of considerable importance due to approximated character of diameter from this method.

The surface analyses done for pure  $\text{CaCO}_3$  by the use of sorptometric analysis (Sorptomat ASAP 2405, Micrometrics Inc.) indicated on physical adsorption of nitrogen and the formation of multimolecular adsorption layer at the adsorbent surface. The specific surface area calculated for calcite crystals from BET isotherm was equal to  $23.7 \text{ m}^2/\text{g}$  ( $\pm 0.1 \text{ m}^2/\text{g}$ ) (Fig. 4). The presence of hysteresis loop of adsorption–desorption curves gave information that

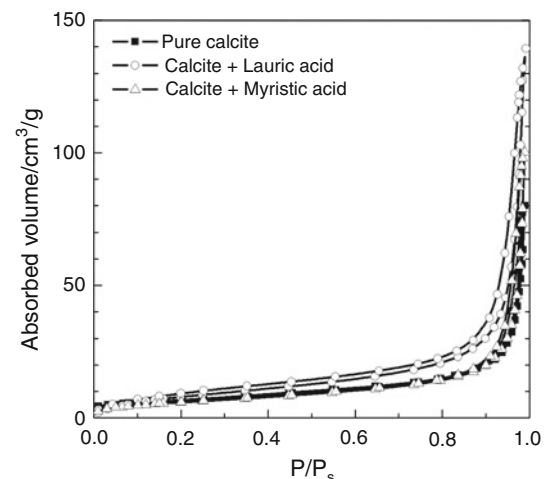


**Fig. 4** Adsorption (desorption) isotherms BET for pure calcite and fatty acids coated calcite

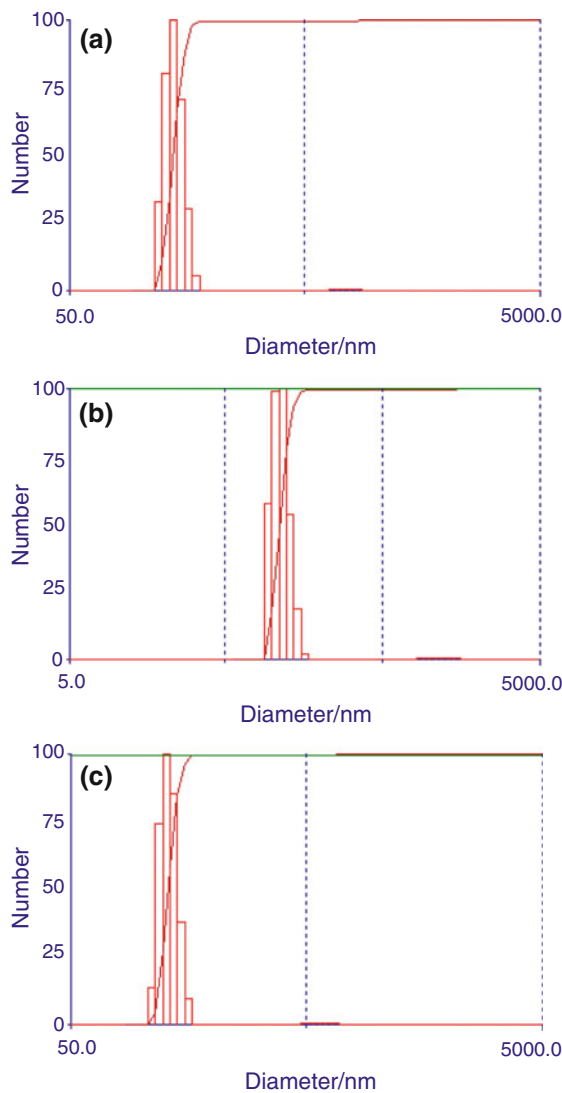


**Fig. 5** Particles size distribution from the DLS method for  $\text{CaCO}_3$  cover by lauric acid: **a** concentration for 0.5 of monolayer (mean diameter 140 nm), **b** concentration for monolayer (mean diameter 111 nm), **c** concentration for 1.5 of monolayer (mean diameter 131 nm)

analyzed powders surface was porous and observed mesopores of size from 2 to 50 nm came from the coalescence of calcite crystallites [23]. For 120 rpm, the mean pores size was equal to 15.1 nm and the volume of micropores increased compared to lower mixing rate (30 rpm) [23].

#### Surface structure of $\text{CaCO}_3$ covered by fatty acids

As it was mentioned, the obtained  $\text{CaCO}_3$  particles were covered by fatty acids. The size distributions of those particles in suspensions examined by Zeta Plus instrument (Brookhaven Instruments Co.) are shown in Fig. 5 for lauric acid and Fig. 6 for myristic acid. Similar to the results obtained for pure  $\text{CaCO}_3$ , the particles covered by

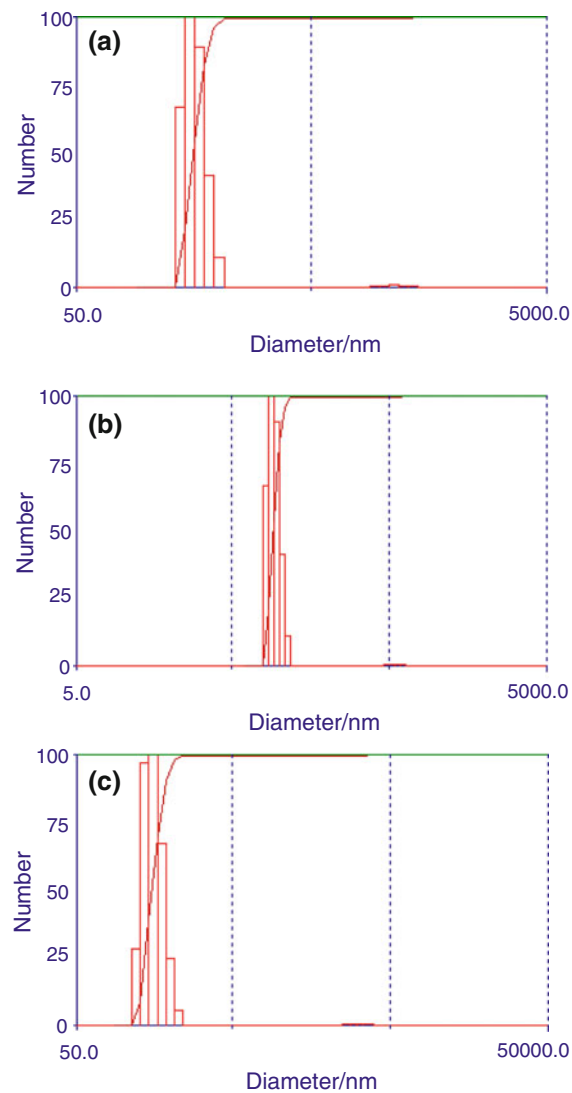


**Fig. 6** Particles size distribution from the DLS method for  $\text{CaCO}_3$  cover by myristic acid: **a** concentration for 0.5 of monolayer (mean diameter 167 nm), **b** concentration for monolayer (mean diameter 91 nm), **c** concentration for 1.5 of monolayer (mean diameter 154 nm)

both fatty acids are also characterized by very narrow particles size distribution with a smaller mean diameter equal to 187 nm ( $\pm 5$  nm) for lauric acid and 91 nm ( $\pm 5$  nm) for myristic acid for monolayer concentration of fatty acids. The smaller diameter of the aggregates can be explained by the fact that fatty acids play here role of anti-aggregating agent as surfactants—this agrees with our previous investigations [23].

The surface analyses done for fatty acids coated  $\text{CaCO}_3$  by the use of sorptometric analysis (Sorptomat ASAP 2405, Micrometrics Inc.) indicated, as in the case of pure calcite, on physical adsorption of nitrogen and the formation of multimolecular adsorption layer at the adsorbent surface. The specific surface area calculated from BET

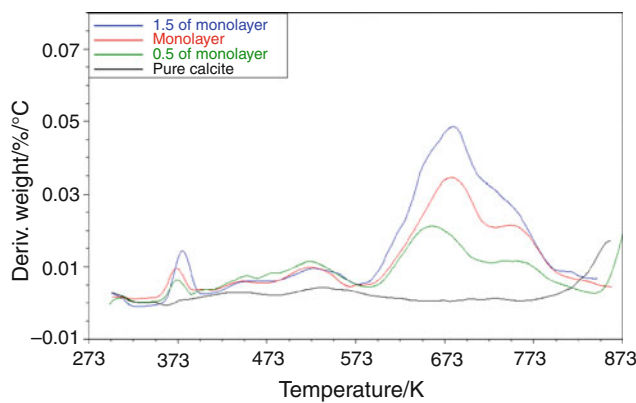


**Fig. 7** TG traces for  $\text{CaCO}_3$  cover by lauric acid

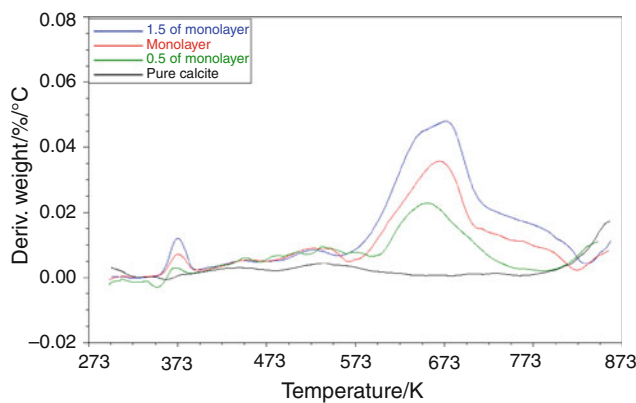


**Fig. 8** TG traces for  $\text{CaCO}_3$  cover by myristic acid

isotherm was equal to 31.3 and  $28.3 \text{ m}^2/\text{g}$  ( $\pm 0.1 \text{ m}^2/\text{g}$ ) for dodecanoic and tetradecanoic acid, respectively (Fig. 4). The higher, compared to the pure calcite, specific surface area obtained for fatty acids coated  $\text{CaCO}_3$  fully corresponds to the stabilization of pure calcite crystallites and protection against particles agglomeration. The particles diameter corresponding with such surface area, under assumption that the particles are cubes is equal to 90 nm ( $\pm 3 \text{ nm}$ ) for pure calcite and 71 nm ( $\pm 3 \text{ nm}$ ) for myristic acid-coated particles.

The crucial problem is concerned with the structure and amount of fatty acids adsorbed on the calcite surface. We have used the thermogravimetric method (TG) for analysis

of calcite powder treated with different amounts of fatty acids. It allows for adsorbed lipid layers morphology studies as well as for interface chemical composition and quantity examination [31–34]. Our investigations have been performed for three different concentrations of the studied fatty acids by the use of 951 TGA Du Pont Instruments in temperature range from 298.15 to 898.15 K. The obtained TG traces are shown in Fig. 7 for lauric acid and in Fig. 8 for myristic acid. The traces on both figures have similar shape and show several mass loss temperatures of calcite powders coated with the acids. Looking at them closely one can distinguish four different peaks for high (1.5 of monolayer) concentration and three peaks for lower (0.5 of monolayer and monolayer) concentration of fatty acids (Figs. 7, 8). The first peak which appears at 373.15 K, and is visible for all concentrations of both acids is connected with water vaporization. The second peak which is also visible for all concentrations of the acids is connected with chemisorption on calcite surface. It appears at 685.15 K for lauric acid (Fig. 7) and at 663.15 K for myristic acid (Fig. 8). The third peak connected with salt formation is visible for all concentration in the case of lauric acid (formation of calcium laurate at 748.15 K; Fig. 7) and for higher (monolayer and 1.5 of monolayer) concentration of myristic acid (formation of calcium myristate at 718.15 K; Fig. 7). Finally, fourth peak is connected with formation of local bilayer and appears only for high (1.5 of monolayer) concentrations for both fatty acids: at 653.15 K (local bilayer of lauric acid molecules) lauric acid and at 628.15 K (local bilayer of myristic acid molecules) for myristic acid.

The amount of water and fatty acid species forming layers on calcite have been calculated from TG data after peaks deconvolution and summarized in Tables 1 and 2 for lauric and myristic acid, respectively.

It is clearly seen that for both fatty acids, the best results have been obtained for concentration of the acids equal to the formation of monolayers. In these cases, the calcite was covered with highest (3.44% for lauric and 3.48% for myristic acid) efficiency only by the monolayers. Also, for lower fatty acid concentration (0.5 of monolayer; Tables 1 and 2), only monolayers were formed on the calcite surface, but the efficiency was much lower (2.04% for lauric

**Table 1** The amount of water and lauric acid species forming layers on calcite

Lauric acid concentration	Mass/%			
	$\text{H}_2\text{O}$ Peak at 373.15 K	Lauric acid chemisorption Peak at 685.15 K	Calcium laurate Peak at 748.15 K	Local bilayer of lauric acid Peak at 653.15 K
0.5 of monolayer	$0.15 \pm 0.002$	$2.04 \pm 0.020$	$0.95 \pm 0.010$	–
Monolayer	$0.27 \pm 0.003$	$3.44 \pm 0.034$	$1.55 \pm 0.015$	–
1.5 of monolayer	$0.39 \pm 0.004$	$2.95 \pm 0.030$	$1.74 \pm 0.017$	$2.01 \pm 0.020$

**Table 2** The amount of water and myristic acid species forming layers on calcite

Myristic acid concentration	Mass/%			
	H <sub>2</sub> O Peak at 373.15 K	Myristic acid chemisorption Peak at 663.15 K	Calcium myristate Peak at 718.15 K	Local bilayer of myristic acid Peak at 628.15 K
0.5 of monolayer	0.22 ± 0.002	2.29 ± 0.023	—	—
Monolayer	0.32 ± 0.003	3.48 ± 0.035	0.65 ± 0.007	—
1.5 of monolayer	0.84 ± 0.008	3.10 ± 0.031	1.27 ± 0.013	1.65 ± 0.017

and 2.29% for myristic acid). In the case of higher fatty acid concentration (1.5 of monolayer; Tables 1 and 2), both monolayers and local bilayers of fatty acids molecules are formed on the calcite surface.

## Conclusions

The presented method allows for production of very stable and ordered CaCO<sub>3</sub> crystallites, which can be further covered *in situ* by fatty acids. It was found that single crystallite size estimated from Scherrer equation (XRD measurements) was about 30 nm ( $\pm 3$  nm). Such particle diameters were seen on the SEM micrographs. Sedimentation observation proved the aggregation of those nanometric particles which start to sediment after reaching appropriate size.

The testing of particles size in suspension by the use light scattering methods gave higher diameters values, but showed that the submicrometric aggregates are almost monodispersed. The fatty acid monolayer formed *in situ* at precipitated calcite prevents form crystallites aggregation and decreases particles mean diameter from 219 nm ( $\pm 5$  nm) for pure calcite up to 111 nm ( $\pm 5$  nm) for calcite/lauric acid systems and 91 nm ( $\pm 5$  nm) for calcite/myristic acid composites. The surface analyses done for fatty acids coated CaCO<sub>3</sub> indicated that the specific surface area calculated from BET isotherm was higher compared to the pure calcite. This also proofs the anti-aggregating properties and stabilization of freshly precipitated by fatty acid adsorption resulting in powders specific surface developing.

Experimental results obtained for the fatty acids coated calcite by the use of thermogravimetric method confirmed its applicability for proper analysis of calcite powder treated with different amounts of the acids and allows for determining of the optimum concentration of fatty acids needed for maximal covering of calcite surface by their monolayers.

**Acknowledgements** This study was carried out within the Ministry of Science and Higher Education Research Project No. 1206/GDR/2007/03.

## References

- Spanos N, Koutsoukos PG. Kinetics of precipitation of calcium carbonate in alkaline pH at constant supersaturation. Spontaneous and seeded growth. *J Phys Chem B*. 1998;102:6679–84.
- Rigopoulos S, Jones A. Modeling of semibatch agglomerative gas–liquid precipitation of CaCO<sub>3</sub> in a bubble column reactor. *Ind Eng Chem Res*. 2003;42:6567–75.
- Schlomach J, Quarch K, Kind M. Investigation of precipitation of calcium carbonate at high supersaturations. *Chem Eng Technol*. 2006;29:215–20.
- Sohnel O, Mullin JW. Precipitation of calcium carbonate. *J Cryst Growth*. 1982;60:239–50.
- Reddy MM, Nancollas GH. The crystallization of calcium carbonate: IV. The effect of magnesium, strontium and sulfate ions. *J Cryst Growth*. 1976;35:33–8.
- Kazmierczak TF, Tomson M, Nancollas GH. Crystal growth of calcium carbonate: a controlled composition kinetic study. *J Phys Chem*. 1982;86:103–5.
- Jung T, Kim WS, Choi CK. Effect of monovalent salts on morphology of calcium carbonate crystallized in Couette–Taylor reactor. *Cryst Res Technol*. 2005;40:586–92.
- Dindore VY, Brilman DWF, Versteeg GF. Hollow fiber membrane contactor as a gas–liquid model contactor. *Chem Eng Sci*. 2005;60:467–79.
- Kitano Y, Park K, Hood DW. Pure aragonite synthesis. *J Geophys Res*. 1962;67:4873–4.
- Chen JF, Wang YH, Guo F, Wang XM, Zheng Ch. Synthesis of nanoparticles with novel technology: high-gravity reactive precipitation. *Ind Eng Chem Res*. 2000;39:948–54.
- Cafiero LM, Baffi G, Chianese A, Jachuck RJ. Process intensification: precipitation of barium sulfate using a spinning disk reactor. *Ind Eng Chem Res*. 2002;41:5240–6.
- Feng B, Yonga AK, An H. Effect of various factors on the particle size of calcium carbonate formed in a precipitation process. *Mater Sci Eng A*. 2007;445–446:170–9.
- Montes-Hernandez G, Renard F, Geoffroy N, Charlet L, Pironon J. Rhombohedral calcite precipitation from CO<sub>2</sub>–H<sub>2</sub>O–Ca(OH)<sub>2</sub> slurry under supercritical and gas CO<sub>2</sub> media. *J Cryst Growth*. 2007;308:228–36.
- Judat B, Kind M. Morphology and internal structure of barium sulfate—derivation of a new growth mechanism. *J Colloid Interface Sci*. 2004;269:341–53.
- Chakraborty D, Bhatia SK. Formation and aggregation of polymorphs in continuous precipitation. 2. Kinetics of CaCO<sub>3</sub> precipitation. *Ind Eng Chem Res*. 1996;35:1995–2006.
- Cheng B, Lei M, Yu JG, Zhao X. Preparation of monodispersed cubic calcium carbonate particles via precipitation reaction. *Mater Lett*. 2004;58:1565–70.
- Colfen H, Antonietti M. Mesocrystals: inorganic superstructures made by highly parallel crystallization and controlled alignment. *Angew Chem Int Ed*. 2005;44:5576–91.

18. Banfield JF, Welch SA, Zhang H, Ebert TT, Penn RL. Aggregation-based crystal growth and microstructure development in natural iron oxyhydroxide biominerization products. *Science*. 2000;289:751–4.
19. Wang T, Antonietti M, Colfen H. Calcite mesocrystals: “morphing” crystals by polyelectrolyte. *Chem Eur J*. 2006;12:5722–30.
20. Xu AW, Yu Q, Dong WF, Antonietti M, Colfen H. Stable amorphous  $\text{CaCO}_3$  microparticles with hollow spherical superstructures stabilized by phytic acid. *Adv Mater*. 2005;17:2217–21.
21. Buijnsters PJJA, Donners JJM, Hill SJ, Heywood BR, Nolte RJM, Zwanenburg B, Sommerdijk NAJM. Oriented crystallization of calcium carbonate under self-organized monolayers of amide-containing phospholipids. *Langmuir*. 2001;17:3623–8.
22. Damle C, Kumar A, Sainkar SR, Bhagawat M, Sastry M. Growth of calcium carbonate crystals within fatty acid bilayer stacks. *Langmuir*. 2002;18:6075–80.
23. Kędra-Królik K, Gierycz P. Precipitation of nanostructured calcite in a controlled multiphase process. *J Cryst Growth*. 2009; 311:3674–81.
24. Kędra-Królik K, Gierycz P, Bucki J. Controlled precipitation of  $\text{CaCO}_3$  sub-micro crystals of well-defined structure in a multiphase system. *Arch Metall Mater*. 2006;51:635–9.
25. Kędra-Królik K, Gierycz P. Obtaining calcium carbonate in a multiphase system by the use of new rotating disc precipitation reactor. *J Therm Anal Calorim*. 2006;83:579–82.
26. Klug HP, Alexander LE. X-Ray diffraction procedures. New York: Wiley; 1974.
27. Mills P, Snabre P. Settling of a suspension of hard spheres. *Europhys Lett*. 1994;25:651–6.
28. Dirksen JA, Ring TA. Fundamentals of crystallization: kinetic effects on particle size distributions and morphology. *Chem Eng Sci*. 1991;46:2389–427.
29. Chen PC, Tai CY, Lee KC. Morphology and growth rate of calcium carbonate crystals in a gas–liquid–solid reactive crystallizer. *Chem Eng Sci*. 1997;52:4171–7.
30. Han YS, Hadiko G, Fuji M, Takahashi M. Effect of flow rate and  $\text{CO}_2$  content on the phase and morphology of  $\text{CaCO}_3$  prepared by bubbling method. *J Cryst Growth*. 2007;276:541–8.
31. Rey FJ, Chamorro O, Gil FJM, Gil JM. Characterization of fatty acid methyl esters by thermal analysis. *J Therm Anal Calorim*. 1993;40:463–73.
32. Osman MA, Suter UW. Surface treatment of calcite with fatty acids: structure and properties of the organic monolayer. *Chem Mater*. 2002;14:4408–15.
33. Giron D. Applications of thermal analysis and coupled techniques in pharmaceutical industry. *J Therm Anal Calorim*. 2002;68: 335–53.
34. Kok MV. Recent developments in the application of thermal analysis techniques in fossil fuels. *J Therm Anal Calorim*. 2008; 91:763–73.